Published by SET Publisher

Journal of Basic & Applied Sciences

ISSN (online): 1927-5129

Theoretical Investigation of the Charge Transport Properties of the DPTTA p-Type Single Crystal to the Ambipolar DPTTA-F_4TCNQ Cocrystal

Zhelin Ding[1], Qiqi Mu[1], Junle Ren[1], Yuyao Li[1], Qiguang Shen[1], Li Zhang[2,*] and Shoufeng Zhang[2,3,*]

[1]*School of Automation, Guangxi University of Science and Technology, Liuzhou 545000, Guangxi, China.*

[2]*School of Electronic Engineering, Guangxi University of Science and Technology, Liuzhou 545000, Guangxi, China*

[3]*Key Laboratory of Ministry of Education of Design and Electromagnetic Compatibility of High Speed Electronic System, Shanghai Jiao Tong University, Shanghai 200240, China*

Article Info:

Keywords:
Ambipolarity,
Charge-hopping model,
D-A complexes.

Timeline:
Received: March 16, 2023
Accepted: April 15, 2023
Published: April 28, 2023

Citation: Ding Z, Mu Q, Ren J, Li Y, Shen Q, Zhang L, Zhang S. Theoretical investigation of the charge transport properties of the DPTTA p-type single crystal to the ambipolar DPTTA-F_4TCNQ cocrystal. J Basic Appl Sci 2023; 19: 29-39.

DOI: https://doi.org/10.29169/1927-5129.2023.19.03

Abstract:

Our research has been conducted on the charge transport properties of the single-crystal DPTTA and the cocrystal DPTTA-F_4TCNQ using the density functional theory coupled with incoherent charge-hopping model. Charge mobility is primarily considered from the combination of reorganization energy and charge transfer integral, which are important parameters in model of the charge-hopping model. The reorganization energy of DPTTA in both single-crystal and cocrystal forms exhibits similar values. Consistent with the properties of super-exchange coupling and direct coupling when under the same type of coupling mechanism, it decreases with increasing distance from the core molecule. We conclude this section by using kinetic Monte Carlo combined with Einstein's equation to derive the charge mobility, and find it to be consistent with the theoretical analysis. In our study, we propose corresponding theoretical guidelines for the rational realization of the ambipolarity of D-A complexes, hoping to contribute to the understanding and rational design of the basic mechanism of D-A complexes.

*Corresponding Author
E-mail: zhangli@gxust.edu.cn, zhangsf@gxust.edu.cn

1. INTRODUCTION

Due to their low price and good carrier mobility, organic semiconductors have been widely studied [1-3]. Ambipolar organic semiconductors can transport holes and electrons simultaneously in organic field-effect transistors (OFETs) [4], which is more advantageous than the use of *n*-type (electronic transport) or *p*-type (hole transport) organic semiconductors [5]. As a result, the use of ambipolar organic materials in organic light-emitting transistors (OLETs) [6, 7] and organic photovoltaics (OPVs) [8] is developing.

There are several ways to achieve ambipolar, the first one is single-crystal [9-12]. Single-crystal ambipolar organic semiconductor is component with some molecules. It can simultaneously transport electronic and hole using molecule HOMO and LUMO. Heterojunction structures [13-15] are another method to realize ambipolarity. Guo *et al*. [16] in 2021 used hexadecafluorophthalocyanine (F_{16}CuPc) to combine 2D molecular crystal (2DMC) as a heterojunction to form ambipolar organic field effect transistors. The third method is cocrystal that have two or more component connected by noncovalent interactions in the crystalline [17]. In comparison to the single-crystal, the cocrystal is more amenable to ambipolar realization, which uses donor (D) molecules and accepter (A) molecules to achieve simultaneous hole and electron transport, with the benefits of facile synthesis and broad applicability [18-20]. The use of D-A complexes for ambipolar transport developed rapidly [21] after T. Hasegawa *et al*. [22] reported the behavior of ambipolar transport at low temperatures using complexes of the type BEDTTTF-F_2TCNQ [23]. Li *et al*. [24] in 2013 subsequently presented an overview of the D-A system with DPP as an acceptor to achieve power conversion efficiencies as high as 6.05% in OPVs and high mobility on OFETs. Recently Balambiga *et al*. [25] successfully used Picene and PTCDI to achieve ambipolar transport in OFETs. As well as a lot of D-A complexes to form ambipolar materials such as Perylene-TCNQ [26], DBTTF-TCNQ [27] and Co-TPP-C60 [28] are good ambipolar D-A complexes. These results demonstrate that using cocrystal to realize ambipolar organic semiconducting is an effective approach.

However, the cocrystal for ambipolar semiconductors is confronted with various challenges. For example, the basic mechanism of co-crystallization is pointedly ambiguous, it limited cocrystal devloped. In this paper we try several studies of the charge transport properties have been performed for cocrystal [29-32]. The study of cocrystal can be found by considering the energy levels, the transfer integral, and the effects of orbitals. Here, we compute frontier molecular orbitals, reorganization energies, charge transfer integrals, and anisotropy of carrier mobility of single-crystal DPTTA (meso-diphenyl terathia[22]annulene[2,1,2,1]) and the cocrystal DPTTA-F_4TCNQ (DPTTA=meso-diphenyl terathia[22]annulene[2,1,2,1], F_4TCNQ=fluorinated derivarives of 7,7,8,8,-teracyanoquinodimethane), with the expectation of providing some assistance in the design of D-A complexes [33]. TCNQ [34] is an extended *n*-type material with good planarity, forming D-A complexes that are more likely to form stacks face-to-face in order to produce good super-exchange coupling [29]. F_4TCNQ is the product after replacing TCNQ with four F atoms, which has a better electron-accepting capability compared to TCNQ [35]. However, the theoretical part of cocrystal DPTTA-F_4TCNQ has not been reported much. The aim of this study was to investigate the charge transport properties of DPTTA and DPTTA-F_4TCNQ in order to compare the change in charge transport properties of ambipolar D-A complexes by incorporating F_4TCNQ. Which are discussed primarily from the Marcus theory in terms of the reorganization energy and the transfer integral, which are important influencing factors. The change in reorganization energy of DPTTA molecules after the incorporation of F_4TCNQ molecules is obtained in Section 3.2 and the change of transfer integral in Section 3.2, from these two parameters, we obtain the rational design guidelines of D-A complexes.

2. METHODOLOGICAL APPROACH

Density functional theory (DFT) calculations were carried out for both the DPTTA and the DPTTA-F_4TCNQ. These are rates of intermolecular charges using the Marcus equation [36]:

$$K = \frac{|V|_2}{\hbar}\left(\frac{\pi}{\lambda k_B T}\right)^{1/2} \exp\left(-\frac{\lambda}{4k_B T}\right) \quad (1)$$

Where V represents the transfer integral between the initial state and the final state. We used direct coupling method in this paper to calculated transfer integral and then V is $< \psi_i^0 | F | \psi_j^0 >$ Where *F* represents the Fock operator

$$F = SC\varepsilon C^{-1} \quad (2)$$

Here S denotes the intermolecular overlap matrix, C is the coefficient of the dimer Kohn-Sham orbital and ε

denotes the energy of the dimer Kohm-Sham orbital. λ is reorganization energy and we have two models to calculate. The first one is the adiabatic potential method $(\lambda = \lambda_1 + \lambda_2)$ in Figure **S1** (Supporting information) and the second one is normal-model $(\lambda = \sum_j \lambda_j = \sum_j S_j \hbar w_j)$. Here λ_1 is the energy difference between the neutral geometry and charged geometry in the optimal and λ_2 is the energy difference with the charged molecule in two geometries. In the normal-model S_j is Huang-Rhys factor representing the local electronic-phonon coupling, and w_j represent the vibration frequency in the j mode.

Charge mobility calculated by the Einstein equation $u = \frac{eD}{K_B T}$ where e is the charge, K_B is the Boltzmann constant, T is the room temperature with 298K, and D is the charge diffusion coefficient. We used the kinetic Monte Carlo simulations to evaluate D. From y molecule to the z molecule through the f pathway, the charge hops probability is $p_f = \frac{K_{yz}^f}{\sum_f K_{yz}^f}$. The simulation time can be expressed as $\frac{1}{K_{yz}^f}$, where the K_{yz}^f is the charge hopping rate of y molecule to z molecule through the f pathway. The kinetic Monte Carlo simulation randomly selects a random number m between 0 and 1 when $\sum_{f=1}^{j-1} p_f < m \le \sum_{f=1}^{j} p_f$ then the charge hops along the j direction. This method was carried out 2000 times, each time for 10us finally obtain the relationship between the diffusion coefficient D and the mean-square displacement $l(t)^2, D = \lim_{t\to\infty} \frac{l(t)^2}{6t}$ which can be brought into Einstein's equation to derive the charge mobility.

For both DPTTA and DPTTA-F_4TCNQ, we use the program Gaussian16 [37] to compute the geometry optimization and the frequency. The DPTTA single-crystal and DPTTA-F_4TCNQ cocrystal reorganization energy geometry optimization, vibrational mode analysis, and transfer integral calculations are all done at the B3LYP/6-31G(d,p) level. All calculations of charge mobility using the MOMAP software package [38]. Each kinetic Monte Carlo runs 2000 simulations and 1 ms of simulation time for each mobility computation.

3. RESULTS AND DISCUSSION

3.1. Crystal Structures

All of the crystal structure data used in this article are taken from the Cambridge Crystallographic Data

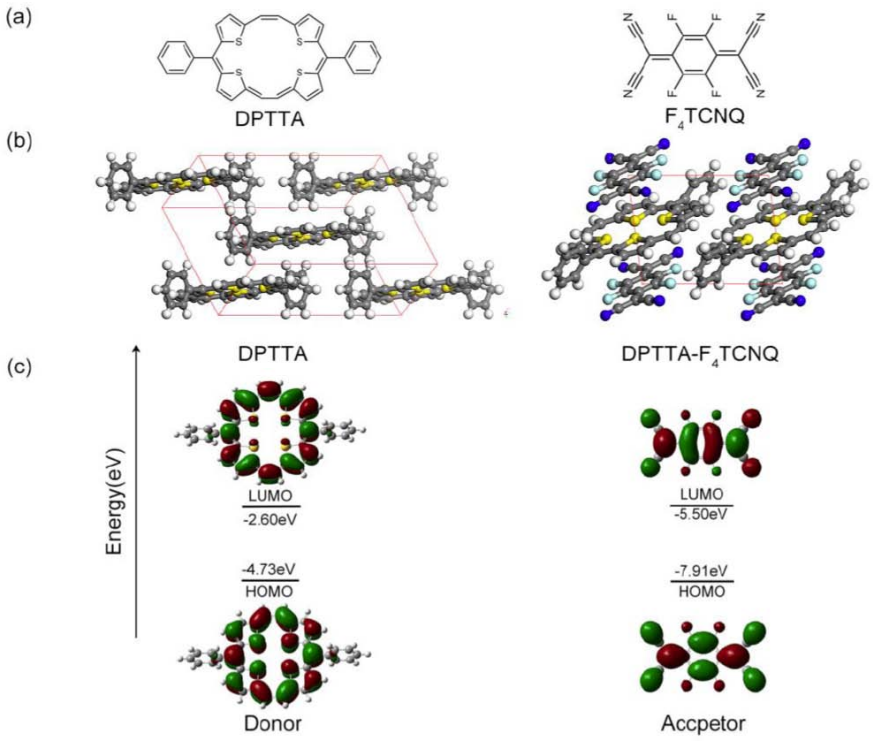

Figure 1: (**a**). Chemical structure of DPTTA and F_4TCNQ. (**b**). Crystal structure of DPTTA single crystal and DPTTA-F_4TCNQ cocrystal. (**c**). Energy level diagram for DPTTA and F_4TCNQ.

Centre (CCDC). In the case of the DPTTA single-crystal, the space group is C2/m, the DPTTA-F_4TCNQ cocrystal belong to the P1, and the ratio of the DPTTA-F_4TCNQ complexes is 1:1. Depending on the specific search system, one finds that the number of adjacent molecules between DPTTA and F_4TCNQ in cocrystal are not the same, which will be described in detail in the next section on the transfer integral for the charge transport properties.

For Figure **1b** DPTTA single crystal structure we find that the molecular stacking is 2D brickwork stacking not like the DPTTA-F_4TCNQ cocrystal is face-to-face stacking. The reason why DPTTA-F_4TCNQ cocrystal can make D-A face-to-face stack is F_4TCNQ molecular doesn't have benzene ring influence. This indicates that DPTTA-F_4TCNQ cocrystal may produce good charge mobility due to good stacking. But the specific needs to be considered from a combination of transfer integral and reorganization energy. We will explain the specific effects of this stacking pattern on charge mobility in the next two sections. In Figure **1c**, we see that the HOMO and LUMO orbitals for DPTTA are primarily in the conjugated backbone but in F_4TCNQ the orbitals spread evenly on the molecule. In fact, the calculation shows that the HOMO and LUMO orbitals of the DPTTA molecule have a significant overlap with the molecular orbitals of F_4TCNQ, primarily between the conjugated backbones and the four S-atoms. This suggests that the DPTTA-F_4TCNQ cocrystal could theoretically exhibit good charge transport properties, and the carrier mobility results are expected to be improved. As a donor DPTTA has a large ionization energy of -4.73 eV and the electron affinity for F_4TCNQ is -5.50 eV are very close to one another. For HOMO-LUMO bandgap of DPTTA is 2.13 eV and F_4TCNQ is 2.41 eV have a similar HOMO-LUMO bandgap.

3.2. Reorganization Energy Analyze

In terms of the charge transport properties of DPTTA and DPTTA-F_4TCNQ, the calculation of the reorganization energy is an extremely important assessment factor. For the reorganization energy λ we mainly discuss it into two parts, the external reorganization energy and the internal reorganization energy. The external reorganization energy is the interaction between molecules, this part has little influence on the hopping model and the calculation is relatively difficult, so we consider the internal reorganization energy of the molecule. We calculated the reorganization energy of F_4TCNQ and DPTTA molecules using both the adiabatic potential energy surface method and the normal model method. In Figure **2**, we present a comparison of the dispersion of duschinsky rotation matrices with respect other models.

In Figure **2** DPTTA is discrete and F_4TCNQ is linear minds normal-model does not applicable to DPTTA but suitable to F_4TCNQ. As depicted in Table **1**, there exists a considerable difference between the reorganization energies of the DPTTA molecule calculated using the adiabatic potential energy surface method and the normal model method. This discrepancy can be attributed to the unsuitability of the normal model method for calculating the reorganization energy of the DPTTA molecule. Moreover, this validates the discreteness of the duschinsky rotation matrix of the DPTTA molecule presented in Figure **2**. In our calculation, the DPTTA molecular has a smaller λ_e (162 meV) than the F_4TCNQ molecular (which has a λ_e value of 256 meV), while the λ_h value of DPTTA (201 meV) is larger than the λ_h value of F_4TCNQ (which is157 meV). This implies that DPTTA molecules may exhibit superior performance for hole transport, whereas F_4TCNQ molecules may be more adept at

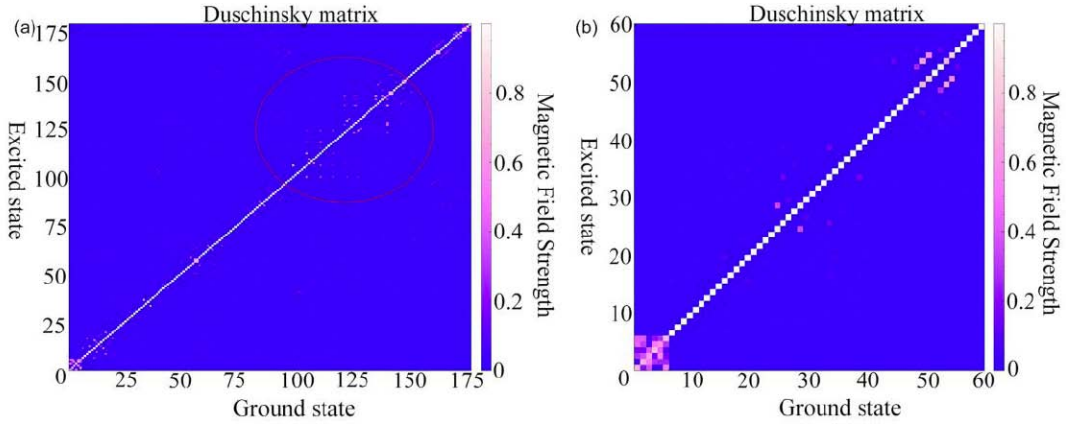

Figure 2: (**a**), (**b**). Duschinsky rotation matrix of DPTTA and F_4TCNQ in ground state.

Table 1: Reorganization energy of adiabatic potential energy method and normal model method for single-crystal DPTTA and cocrystal DPTTA-F_4TCNQ (meV). (all calculate in b3lyp 6-31g(d,p) level)

	Compared	aP (λ_e)	aP (λ_h)	NM(λ_e)	NM(λ_h)
Single-crystal	DPTTA	161.98	201.01	262.79	725.66
cocrystal	DPTTA	161.93	200.93	261.34	715.73
	F4TCNQ	255.60	156.65	256.64	157.18

electron transport. In particular, the DPTTA molecule demonstrates excellent P-type hole transport capabilities with a remarkably low hole reorganization energy, which promotes efficient hole transport. It's worth noting that the difference between the hole reorganization energy of DPTTA molecules (39 meV) and the electron reorganization energy (201 meV) is relatively small and not considered significant.

When analyzed in terms of reorganization energy, ambipolar transport is achievable in DPTTA single crystals, with both types of carriers reaching similar values. However, electronic coupling is another factor that significantly affects the carrier mobility of the crystal. This effect on carrier mobility plays a crucial role in establishing DPTTA as a good P-type organic semiconductor material based on experimental measurements. Unlike DPTTA molecules, where the hole and electron reorganization energies do not differ much, F_4TCNQ is unable to form an ambipolar single crystal due to its larger hole reorganization energy (99meV) difference with electron reorganization energy). In practical applications, F_4TCNQ is widely used as a good n-type material due to its excellent planarity and is often seen in D-A eutectic as an acceptor molecule.

For Figure **3** we first compare Figure **3a** and **b** to find that the major changes in the F_4TNCQ occur in the mid-frequency region. Figure **3c**, **d** shows the F_4TNCQ reorganization energy in the neutral state and anion state. Special attention for (a) and (c) they are F_4TNCQ neutral states for calculating hole and electronic. In (a) have two maximum values is 1509.2 cm^{-1} and 1710.62 cm^{-1} but in (c) only one maximum value in 1509.2 cm^{-1}. The low-frequency reorganization energy for the F_4TCNQ molecule was found to arise primarily from the relative motion of the cyano group, and the N atom starts to stretch. The intermediate-frequency reorganization energy arises from the stretching motion of the carbon-carbon double bond as well as from the movement up and down the benzene ring. The relaxation of this structure leads to the reorganization energy of F_4TCNQ and occurs mainly on the more stable cyano and benzene rings. So the value of the final reorganization energy is not very high. The low-frequency electron reorganization energy in F_4TCNQ is mainly caused by the hydrogen group. In contrast, the

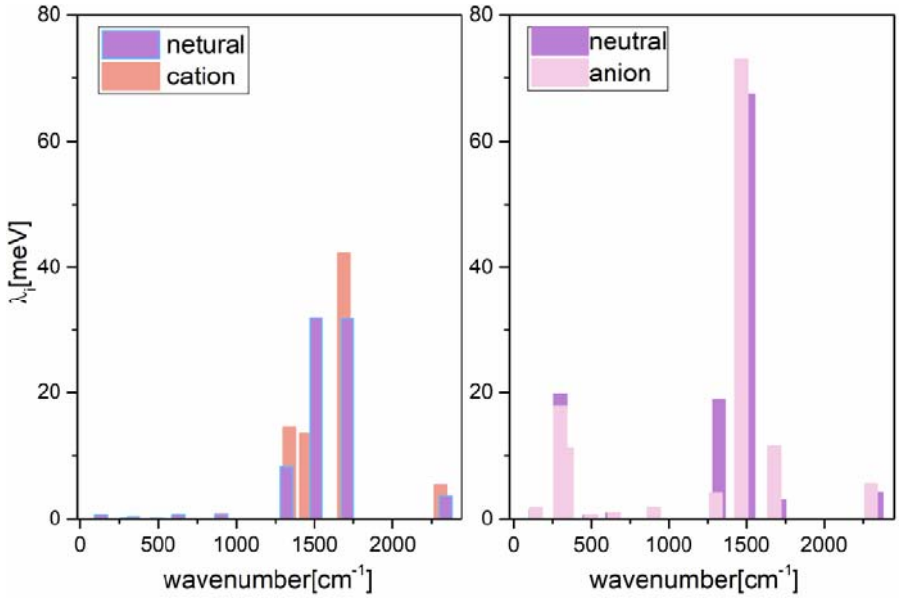

Figure 3: (**a**). The reorganization energy contribution of F_4TCNQ in the ground state and cation state in each vibrational mode. (**b**). Reorganization energy contribution of F_4TCNQ molecule in the ground state and anion state.

stretching of the central benzene ring is the primary factor influencing the hole reorganization energy. Although reorganization energy exhibits more low-frequency regions, there is no significant difference in structural relaxation between the neutral and anionic states. The final electron reorganization energy is lower than that of the hole reorganization energy. To regulate reorganization energy, we can minimize the relative motion of the central benzene ring and increase its skeleton rigidity to achieve a smaller reorganization energy. One possible approach for improving reorganization energy is to reduce the influence of the hydrogen group on electron reorganization energy.

3.3. Transfer Integrals

In the previous section, we have described the reorganization energy of DPTTA and F_4TCNQ. Another important influence on charge transport model is transfer integral, for the transfer integral in cocrystal has a large change and we shall discuss this in detail in this section.

The carrier (hole/electron) transport pathways of the DPTTA single crystal and the DPTTA-F_4TCNQ cocrystal are shown in Figure **4**. It can be found that DPTTA in both the single crystal and cocrystal the transport pathways changed from 12 to 18. For D-A complexes, one can also directly calculate the effective electronic coupling by applying this equation. Figure **5a**, **b**, **c** are used to obtain the calculated electronic coupling results absolute value for the complexes of DPTTA-F_4TCNQ with DPTTA (F_4TCNQ) as the core molecule for the surrounding molecule (All data in supporting information S3). Figure **5a** shows the hole/electron transfer integrals calculated by the molecule DPTTA under the trajectory indicated in Figure **4a**, it can be concluded that the single-crystal transfer integral of DPTTA is consistent with the relationship between the distance and the intensity of the transfer integral. We can see that the transfer integral absolute value of the hole (electron) decreases as the distance is increased. In the cocrystal, this situation is different in that the distance in the path from P1 to P18 is constantly increasing, but the transfer integral of holes (electrons) does not decrease with the distance increase. This difference is evident in the paths P11, P12, P15 and P16 pathways, where the distances of P11 and P12 have increased by 0.48 Å compared to P10, P11, but the hole (electron) transfer integral has increased more than four times from 6.87 meV to -25.03 meV we believe that the mechanism of

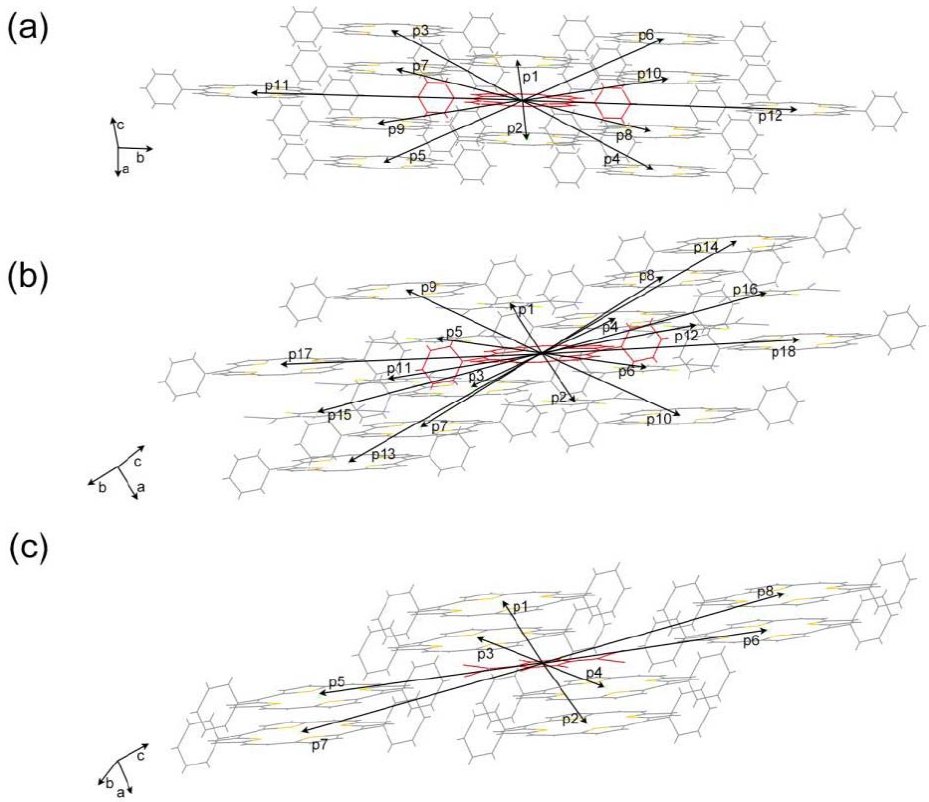

Figure 4: (**a**), (**b**). The carrier transport path of DPTTA molecule in single crystal and cocrystal (**c**). The carrier transport path of F_4TCNQ molecule in DPTTA-F_4TCNQ cocrystal.

super exchange is occuring. While the stacking angle of the complexes, the overlapping area, and the stacking distance all have some influence on the transfer integral. The same conclusion can also be drawn from P15 and P16 when compared to P13 and P14. As the distance increases but the value of the transfer integral doesn't decrease but gets larger. As this is an interesting phenomenon, we searched along the trajectory in Figure **4** and found that P1, P2, P5, P6, P11, P12, P15, and P16 belong to the charge transfer of the effective orbital couplings. However, it is only in the four paths of P11, P12, P15 and P16 that it can be clearly found that the charge transfer integral has a greater increase with respect to the other paths. P1 and P2 belong to the electronic coupling under the direct exchange mechanism between D/D due to the transfer integrals we have calculated satisfying the direct exchange mechanism. Furthermore, we found that the D/A electronic coupling between the F_4TCNQ molecule and the DPTTA molecule is dominated by the superexchange mechanism, as evidenced by paths P11, P12, P15, and P16. The good planarization of the F_4TCNQ molecule plays an important role in molecular orbital formation, contributing to the molecule's strong bonding and antibonding effects, which result in the intermolecular centers moving farther apart. This leads to a good charge transfer integral value due to molecular orbitals and superexchange coupling. We speculate that the charge transfer integral values in DPTTA single crystals follow the distance after the formation of eutectic by reference F_4TCNQ molecules. The superexchange mechanism affects some paths in DPTTA single crystals, resulting in relatively large charge transfer integrals at near-molecular center distances. This phenomenon is closely related to the bonding mechanism of molecular orbitals and the good π-π stacking due to planarization.

From Figure **5a**, we can find the direct exchange mechanism and the super-exchange mechanism. The P17 and P18 paths have larger values of the charge transfer integrals than the P13 and P14 paths. We found that the molecular positions of both the P17 and P18 pathways were in a relatively parallel state, with the centers of the two molecules widely separated but the two conjugated skeletons relatively close together (supporting information S3). The HOMO (LUMO) orbital of the DPTTA molecule is concentrated primarily on the conjugated backbone. The centers of the molecules are parallel, but the centers are farther apart, but the distance of the conjugated backbone is relatively close, and the coupling of the two orbitals is more evident. According to our analysis, P17 is located farther from the molecular center compared to P13 and P14 but exhibits a higher charge transfer integral value. The presence of side chain benzene rings in DPTTA molecules in a single crystal environment can alter the molecular stacking and enhance charge transfer properties. However, when DPTTA single crystals are doped with F4TCNQ molecules, the absence of side chain benzene rings in F4TCNQ leads to a reduced face-to-face stacking distance between molecules. This

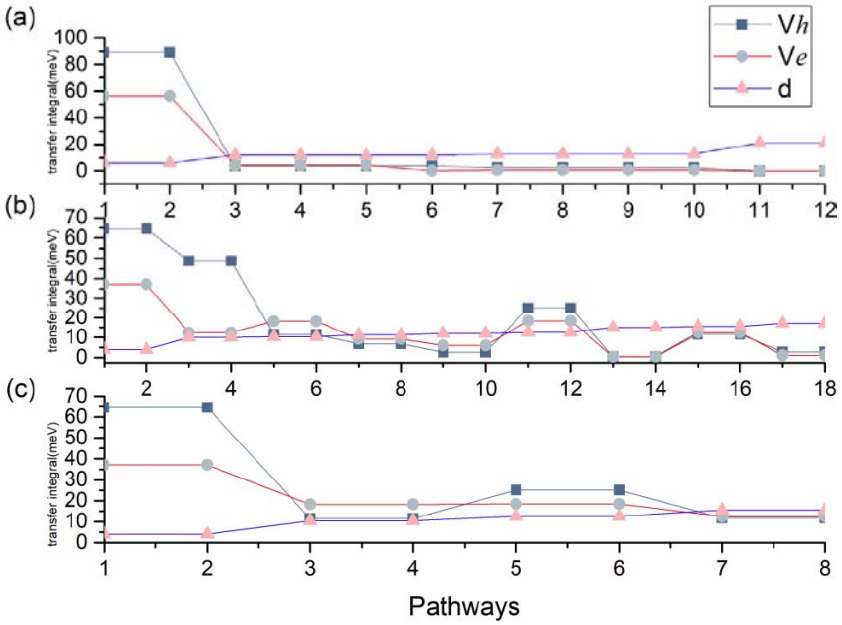

Figure 5: The transfer integral absolute value of transfer pathways for DPTTA molecule in single crystal (**a**) and cocrystal (**b**). F_4TCNQ (**c**) molecule transfer integral absolute value in cocrystal.

reduces the interaction between benzene rings and results in a smaller face-to-face stacking distance. Shorter face-to-face stacking distances lead to higher charge transfer integral values, which is observed when considering the charge transfer products of P1 and P2 paths in the eutectic. Our findings show that the charge transfer integrals under the superexchange mechanism are smaller than those under direct coupling. We also conducted a study of the HOMO (LUMO) orbital energy levels in two different environments of DPTTA molecules. Our analysis reveals that in the same single crystal environment, the HOMO (LUMO) orbitals are closer to each other, resulting in a greater electronic coupling strength. After doping DPTTA with F4TCNQ, the HOMO (LUMO) orbital energy levels of F4TCNQ become closer to those of DPTTA. However, the orbital energy level of F4TCNQ differs significantly from the HOMO (LUMO) orbital energy level of DPTTA, explaining the large difference in charge transfer product values.

The Figure **5c** primarily shows the integral of the charge transfer under the trajectory around the F_4TCNQ molecule. In comparison to the DPTTA molecule, there are only twelve adjacent molecules surrounding the F_4TCNQ molecule. It can also be concluded from the data in Figure **5c** that the charge-transfer integral is continuously decreasing with increasing distance. But then an interesting situation came up. Two adjacent molecular positions, P5, P6 and P7, P8, were found after P3 and P4, all of which increased the corresponding distance, but there was no situation in which the charge-transfer integral decreased with increasing distance. The decrease in the charge transfer integral with increasing distance is due to the large orbital overlap of the stacking between the faces, but molecules at path positions P3 and P4 found in parallel (supporting information S3). The F atoms of the F_4TCNQ molecule are in close proximity to the conjugated backbone, and the benzene ring of the side chain of the DPTTA molecule is in close proximity to the cyano moiety of F_4TCNQ. This orbital overlap situation leads to a situation where the P3 and P4 paths have similar molecular center distances but the hole transfer integral is the smallest. In terms of the electron transfer integral, the central distance of the P5 and P6 paths can be found to increase by 2.134 Å compared to the P3 and P4 paths, but instead the charge transfer integral increases by 0.224 meV. In this portion of the data, the relative position of the orbital overlap, both cyano positions of F_4TCNQ at this position can be found to both face the conjugated backbone of DPTTA, formation of greater LUMO orbital coupling, and formation of electron transfer below the P5, P6 path is greater than the P3 and P4 paths.

3.4. Carrier Mobility and Anisotropic Mobility

The two important factors in the Marcus theory, the reorganization energy and the transfer integral, have been analyzed and discussed in detail above the calculation. DPTTA can be found to be 0.08-0.7 $cm^2V^{-1}{}_S{}^{-1}$ with respect to the experimental value, and the hole mobility of 0.0085 $cm^2V^{-1}{}_S{}^{-1}$ has been calculated in this work. The reason for the large difference between our data results and experimental data is that we believe that the experimentally obtained average value of multiple measurements of the device with the largest charge mobility. And our calculation is based on average value of anisotropy.

Above to calculate shows that DPTTA is an ideal P-type material with moderate hole transport properties, but when it is doped with F_4TCNQ, the hole mobility becomes 0.0172 $cm^2V^{-1}{}_S{}^{-1}$, which is almost an organic semiconductor (10^{-8}~10^{0}) [39] the minimum value defined. With the addition of n-type F4TCNQ, the DPTTA is changed from a P-type unipolar material to an ambipolar material, the calculated electron mobility of 0.5572 $cm^2V^{-1}{}_S{}^{-1}$. The reason for such a large band gap between the hole mobility and the electron mobility is primarily due to the fact that the reorganization energy in F_4TCNQ is much smaller than that of the DPTTA molecules. In order to confirm that the D-A complexes formed by DPTTA-F_4TCNQ are ambipolar transport materials, it is of interest to compare the hole and electron mobilities obtained experimentally, but the hole mobility is orders of magnitude smaller than the electron mobility in a strongly nonequilibrium manner.

For the anisotropy of charge mobility we investigated from the xy, xz, yz directions as shown in Figure **6** The cocrystal orientation could not be determined in the experiment [40]. For the xy direction, we can find that DPTTA single crystal hole anisotropy mobility is maximum mobility in 0° and 180°. The maximum mobility becomes 100°/280° when the F_4TCNQ is doped and the biggest value 2 orders of magnitude bigger. For xz direction, DPTTA single crystal anisotropic mobility maximum in 50°/230° yet in cocrystal the hole mobility is anisotropic like electronic mobility. The maximum anisotropic mobility in the yz direction of the DPTTA single crystal as the DPTTA-F_4TCNQ cocrystal becomes 45° and 225°. Thus, we can find that the mobility motion of the DPTTA single

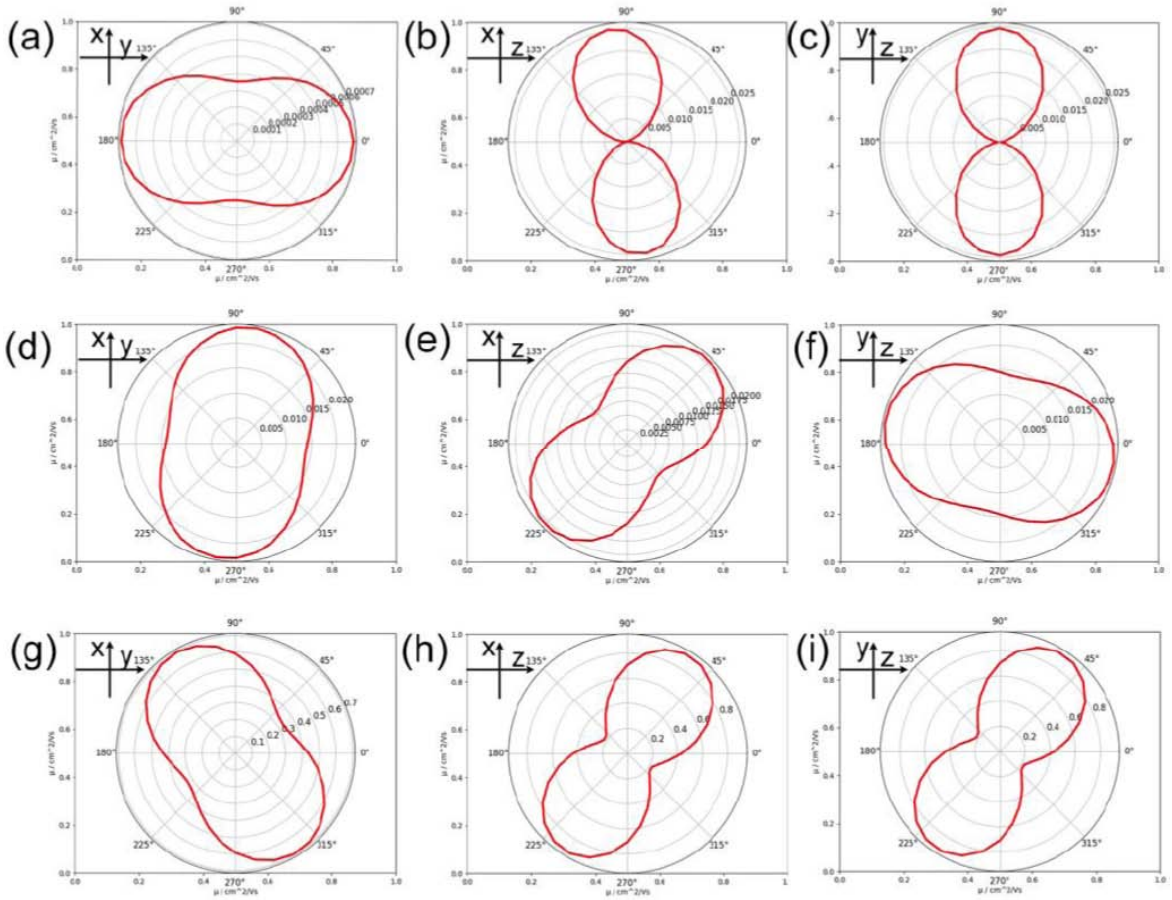

Figure 6: Hole anisotropic charge mobility of DPTTA single crystal ((**a**), (**b**), (**c**)), DPTTA-F_4TCNQ cocrystal ((**d**), (**e**), (**f**)) and DPTTA-F_4TCNQ cocrystal electronic anisotropic charge mobility ((**g**), (**h**), (**i**)) in xy, xz and yz views.

hole is like the hole mobility of the cocrystal however the electronic mobility has different situations. We believe that the direction of anisotropic mobility differ dues to the crystal structure is not the same.

4. CONCLUSIONS

We conclude by completing three pieces of work on the charge transport properties of the single crystal DPTTA and the cocrystal DPTTA-F_4TCNQ, and analyzed the charge transport properties of DPTTA in the single-crystal environment as well as charge transport in the F_4TCNQ doped cocrystal environment. In conclusion, we found in the charge transfer integral, we found that the hole transfer integral of the DPTTA single crystal coincides with a decrease with increasing intermolecular distance, but the hole transfer integral of the DPTTA-F_4TCNQ cocrystal is different, the most obvious one is that the intermolecular center distance of the P11, P12 paths increases but the size is 12 times that of the P9 and P10 paths. We believe that in this case there is a super-exchange coupling. Compared with direct coupling, it is found that the transfer integral provided by the super-exchange coupling mechanism is larger, and super-exchange coupling is the same as direct coupling reduce. In the final analysis of charge mobility, it was found that the anisotropic mobility (supporting information) diffusion of the DPTTA-F_4TCNQ cocrystal was greater than that of the DPTTA single crystal in the three-dimensional case. These results indicate that it is more difficult to achieve directional transport of the cocrystal molecules DPTTA-F_4TCNQ, which will cause a large loss of carriers.

From the analysis of the above results we can put forward a reasonable estimate of the charge mobility optimization. Improve the charge mobility of the DPTTA-F_4TCNQ cocrystal is to reduce the structural relaxation of the side-chain benzene ring or to remove the side-chain benzene ring. The coupling of the super exchange mechanism shows its importance in DPTTA-F_4TCNQ. The premise of increasing the distance between molecular centers is that the super exchange coupling hole transfer integral is approximately 4 times larger than the direct coupling hole transfer integral.

This provides evidence that within the same intermolecular distance the transfer integral under the super exchange coupling mechanism has a larger value than the coupling integral under direct coupling. The second solution to improving mobility is thus to rationally use the super exchange coupling mechanism, in order for the mobility of the cocrystal D-A complexes to increase to a reasonable higher value.

SUPPORTING INFORMATION

The supporting information can be downloaded from the journal website along with the article.

REFERENCES

[1] Bronstein H, Nielsen CB, Schroeder BC, McCulloch I. The role of chemical design in the performance of organic semiconductors. Nature Reviews Chemistry 2020; 4(2): 66-77. https://doi.org/10.1038/s41570-019-0152-9

[2] Zhao W, Ding J, Zou Y, Di C-A, Zhu D. Chemical doping of organic semiconductors for thermoelectric applications. Chemical Society Reviews 2020; 49(20): 7210-7228. https://doi.org/10.1039/D0CS00204F

[3] Wang X, Wang W, Yang C, Han D, Fan H, Zhang J. Thermal transport in organic semiconductors. Journal of Applied Physics 2021; 130(17): 170902. https://doi.org/10.1063/5.0062074

[4] Li S, *et al*. An organic cocrystal based on phthalocyanine with ideal packing mode towards high-performance ambipolar property. Journal of Materials Chemistry C 2022; 10(25): 9596-9601. https://doi.org/10.1039/D2TC01341J

[5] Anthony JE, Facchetti A, Heeney M, Marder SR, Zhan X. n-Type organic semiconductors in organic electronics. Advanced Materials 2010; 22(34): 3876-3892. https://doi.org/10.1002/adma.200903628

[6] Capelli R, Toffanin S, Generali G, Usta H, Facchetti A, Muccini M. Organic light-emitting transistors with an efficiency that outperforms the equivalent light-emitting diodes. Nature Materials 2010; 9(6): 496-503. https://doi.org/10.1038/nmat2751

[7] Dinelli F, *et al*. High-mobility ambipolar transport in organic light-emitting transistors. Advanced Materials 2006; 18(11): 1416-1420. https://doi.org/10.1002/adma.200502164

[8] Yan C, *et al*. Ambipolar-transport wide-bandgap perovskite interlayer for organic photovoltaics with over 18% efficiency. Matter 2022. https://doi.org/10.1016/j.matt.2022.04.028

[9] Liu L, *et al*. Lamellar organic light-emitting crystals exhibiting spectral gain and 3.6% external quantum efficiency in transistors. ACS Materials Letters 2021; 3(4): 428-432. https://doi.org/10.1021/acsmaterialslett.1c00056

[10] Takahashi T, Takenobu T, Takeya J, Iwasa Y, Ambipolar light-emitting transistors of a tetracene single crystal. Advanced Functional Materials 2007; 17(10): 1623-1628. https://doi.org/10.1002/adfm.200700046

[11] Wang Z, *et al*. Reversing interfacial catalysis of ambipolar WSe2 single crystal. Advanced Science 2020; 7(3): 1901382. https://doi.org/10.1002/advs.201901382

[12] De Boer R, *et al*. Ambipolar Cu-and Fe-phthalocyanine single-crystal field-effect transistors. Applied Physics Letters 2005; 86(26): 262109. https://doi.org/10.1063/1.1984093

[13] Hu R, Wu E, Xie Y, Liu J. Multifunctional anti-ambipolar pn junction based on MoTe2/MoS2 heterostructure. Applied Physics Letters 2019; 115(7): 073104. https://doi.org/10.1063/1.5109221

[14] On S, Kim Y-J, Lee H-K, Yoo H. Ambipolar and anti-ambipolar thin-film transistors from edge-on small-molecule heterostructures. Applied Surface Science 2021; 542: 148616. https://doi.org/10.1016/j.apsusc.2020.148616

[15] Lei T, *et al*. Ambipolar Photoresponsivity in an Ultrasensitive Photodetector Based on a WSe2/InSe Heterostructure by a Photogating Effect. ACS Applied Materials & Interfaces 2021; 13(42): 50213-50219. https://doi.org/10.1021/acsami.1c12330

[16] Guo S, *et al*. 2D molecular crystal templated organic p–n heterojunctions for high-performance ambipolar organic field-effect transistors. Journal of Materials Chemistry C 2021; 9(17): 5758-5764. https://doi.org/10.1039/D1TC00715G

[17] Huang Y, Wang Z, Chen Z, Zhang Q. Organic Cocrystals: Beyond Electrical Conductivities and Field-Effect Transistors (FETs). Angewandte Chemie International Edition 2019; 58(29): 9696-9711. https://doi.org/10.1002/anie.201900501

[18] Zhu W, Zhang X, Hu W. Molecular cocrystal odyssey to unconventional electronics and photonics. Science Bulletin 2021; 66(5): 512-520. https://doi.org/10.1016/j.scib.2020.07.034

[19] Sun L, Zhu W, Zhang X, Li L, Dong H, Hu W. Creating organic functional materials beyond chemical bond synthesis by organic cocrystal engineering. Journal of the American Chemical Society 2021; 143(46): 19243-19256. https://doi.org/10.1021/jacs.1c07678

[20] Huang Y, *et al*. Green grinding-coassembly engineering toward intrinsically luminescent tetracene in cocrystals. ACS Nano 2020; 14(11): 15962-15972. https://doi.org/10.1021/acsnano.0c07416

[21] Kulkarni AP, Zhu Y, Babel A, Wu P-T, Jenekhe SA, New Ambipolar Organic Semiconductors. 2. Effects of Electron Acceptor Strength on Intramolecular Charge Transfer Photophysics, Highly Efficient Electroluminescence, and Field-Effect Charge Transport of Phenoxazine-Based Donor−Acceptor Materials. Chemistry of Materials 2008; 20(13): 4212-4223. https://doi.org/10.1021/cm7022136

[22] Hasegawa T, Mattenberger K, Takeya J, Batlogg B. Ambipolar field-effect carrier injections in organic Mott insulators. Physical Review B 2004; 69(24): 245115. https://doi.org/10.1103/PhysRevB.69.245115

[23] Lee J, Han A-R, Yu H, Shin TJ, Yang C, Oh JH. Boosting the ambipolar performance of solution-processable polymer semiconductors via hybrid side-chain engineering. Journal of the American Chemical Society 2013; 135(25): 9540-9547. https://doi.org/10.1021/ja403949q

[24] Li Y, Sonar P, Murphy L, Hong W. High mobility diketopyrrolopyrrole (DPP)-based organic semiconductor materials for organic thin film transistors and photovoltaics. Energy & Environmental Science 2013; 6(6): 1684-1710. https://doi.org/10.1039/c3ee00015j

[25] Balambiga B, Dheepika R, Devibala P, Imran PM, Nagarajan S. Picene and PTCDI based solution processable ambipolar OFETs. Scientific Reports 2020; 10(1): 1-13. https://doi.org/10.1038/s41598-020-78356-5

[26] Vermeulen D, *et al*. Charge transport properties of Perylene–TCNQ crystals: The Effect of stoichiometry. The Journal of Physical Chemistry C 2014; 118(42): 24688-24696. https://doi.org/10.1021/jp508520x

[27] Wu H-D, Wang F-X, Xiao Y, Pan G-B. Preparation and ambipolar transistor characteristics of co-crystal microrods of dibenzotetrathiafulvalene and tetracyanoquinodimethane. Journal of Materials Chemistry C 2013; 1(12): 2286-2289. https://doi.org/10.1039/c3tc30112e

[28] Wakahara T, *et al*. Fullerene/cobalt porphyrin hybrid nanosheets with ambipolar charge transporting characteristics. Journal of the American Chemical Society 2012; 134(17): 7204-7206. https://doi.org/10.1021/ja211951v

[29] Zhu L, Yi Y, Li Y, Kim E-G, Coropceanu V, Brédas J-L. Prediction of remarkable ambipolar charge-transport characteristics in organic mixed-stack charge-transfer crystals. Journal of the American Chemical Society 2012; 134(4): 2340-2347. https://doi.org/10.1021/ja210284s

[30] Zhu L, Yi Y, Fonari A, Corbin NS, Coropceanu V, Brédas J-L. Electronic properties of mixed-stack organic charge-transfer crystals. The Journal of Physical Chemistry C 2014; 118(26): 14150-14156. https://doi.org/10.1021/jp502411u

[31] Hu P, Du K, Wei F, Jiang H, Kloc C. Crystal growth, HOMO–LUMO engineering, and charge transfer degree in perylene-F x TCNQ (x= 1, 2, 4) organic charge transfer binary compounds. Crystal Growth & Design 2016; 16(5): 3019-3027. https://doi.org/10.1021/acs.cgd.5b01675

[32] Geng H, Zheng X, Shuai Z, Zhu L, Yi Y. Understanding the Charge Transport and Polarities in Organic Donor–Acceptor Mixed-Stack Crystals: Molecular Insights from the Super-Exchange Couplings. Advanced Materials 2015; 27(8): 1443-1449. https://doi.org/10.1002/adma.201404412

[33] Zhang J, *et al*. Sulfur-Bridged Annulene-TCNQ Co-Crystal: A Self-Assembled "Molecular Level Heterojunction" with Air Stable Ambipolar Charge Transport Behavior. Advanced Materials 2012; 24(19): 2603-2607. https://doi.org/10.1002/adma.201200578

[34] Menard E, Podzorov V, Hur SH, Gaur A, Gershenson ME, Rogers JA. High-performance n-and p-type single-crystal organic transistors with free-space gate dielectrics. Advanced Materials 2004; 16(23-24): 2097-2101. https://doi.org/10.1002/adma.200401017

[35] Castagnetti N, Masino M, Rizzoli C, Girlando A, Rovira C. Mixed stack charge transfer crystals: Crossing the neutral-ionic borderline by chemical substitution. Physical Review Materials 2018; 2(2): 024602. https://doi.org/10.1103/PhysRevMaterials.2.024602

[36] Marcus RA. Electron transfer reactions in chemistry. Theory and experiment in Protein electron transfer: Garland Science 2020; pp. 249-272. https://doi.org/10.1201/9781003076803-10

[37] Gaussian RA. "1, mj frisch, gw trucks, hb schlegel, ge scuseria, ma robb, jr cheeseman, g. Scalmani, v. Barone, b. Mennucci, ga petersson *et al*., gaussian," Inc., Wallingford CT, 2009; 121: 150-166.

[38] Niu Y, *et al*. MOlecular MAterials Property Prediction Package (MOMAP) 1.0: a software package for predicting the luminescent properties and mobility of organic functional materials. Molecular Physics 2018; 116(7-8): 1078-1090. https://doi.org/10.1080/00268976.2017.1402966

[39] Jiang H, *et al*. Tuning of the degree of charge transfer and the electronic properties in organic binary compounds by crystal engineering: a perspective. Journal of Materials Chemistry C 2018; 6(8): 1884-1902. https://doi.org/10.1039/C7TC04982J

[40] Qin Y, *et al*. Efficient ambipolar transport properties in alternate stacking donor–acceptor complexes: from experiment to theory. Physical Chemistry Chemical Physics 2016; 18(20): 14094-14103. https://doi.org/10.1039/C6CP01509C